SUPPLEMENTAL DATA

Vivek Garg, Anna Stary-Weinzinger, Frank Sachse and Michael C. Sanguinetti

Molecular determinants for activation of human ERG1 potassium channels by 3-nitro-N-(4-phenoxyphenyl) benzamide.

Molecular Pharmacology

Supplementary Figure S1

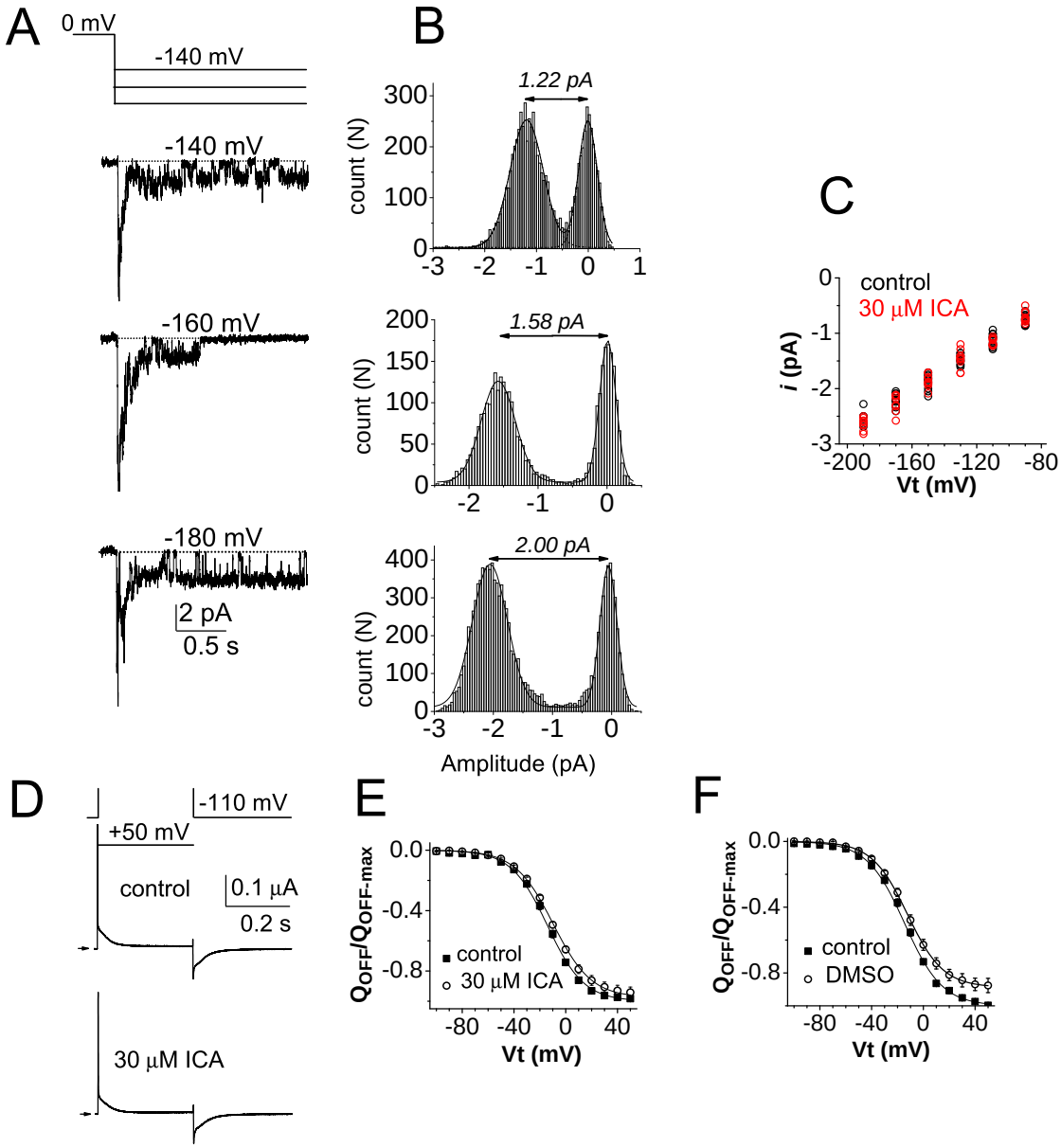

Fig. S1. ICA does not alter single channel conductance or gating currents of hERG1 channels. (A) Example of single channel currents measured from an untreated oocyte. This patch contained several hERG1 channels that rapidly deactivated upon repolarization to the indicated test potential after a 1 s pulse to 0 mV. (B) Amplitude histograms determined from currents shown in panel A, using the period where activity of one single channel was evident. (C) Scattergram of single channel current amplitudes for patches recorded in the absence of drug (black circles, n = 10) plus patches recorded in the presence of 30 μM ICA (red circles, n = 10) in the bathing solution and in the recording pipette. (D) Gating currents measured using COVG in a single oocyte before and after treatment for 20 min with 30 μM ICA. Currents were elicited at a Vt of +50 mV and a return potential of 110 mV. (E) Effect of 30 μM ICA on Q_{OFF}-V relationships normalized to the value at +50 mV under control conditions for each oocyte. Data were fitted with a Boltzmann function (smooth curves). For control, $V_{0.5}$ = 14.0 ± 0.6mV, k = 14.1 ± 0.3 mV; for ICA, $V_{0.5}$ = 9.7 ± 1.0 mV, k = 14.7 ± 0.3 mV (n = 5). Off gating charge (Q_{OFF}) was determined by integration of the OFF gating current measured at 110 mV. The average Q_{OFF} after a pulse to +50 mV was 4.8 ± 1.0 nC for Control and 4.5 ± 0.8 nC after 20 min of ICA. (F) Effect of DMSO (vehicle for ICA) on Q_{OFF}-V relationships normalized to the value at +50 mV under control conditions for each oocyte. For control, V0.5 = 12.3 ± 0.9 mV, k = 13.8 ± 0.3 mV; for DMSO, $V_{0.5}$ = 14.4 ± 0.6 mV, k = 14.6 ± 0.3 mV (n = 4). The average Q_{OFF} after a pulse to +50 mV was 8.5 ± 2.5 nC for Control and 7.6 ± 2.3 nC after 20 min of DMSO.

Supplementary Figure S2

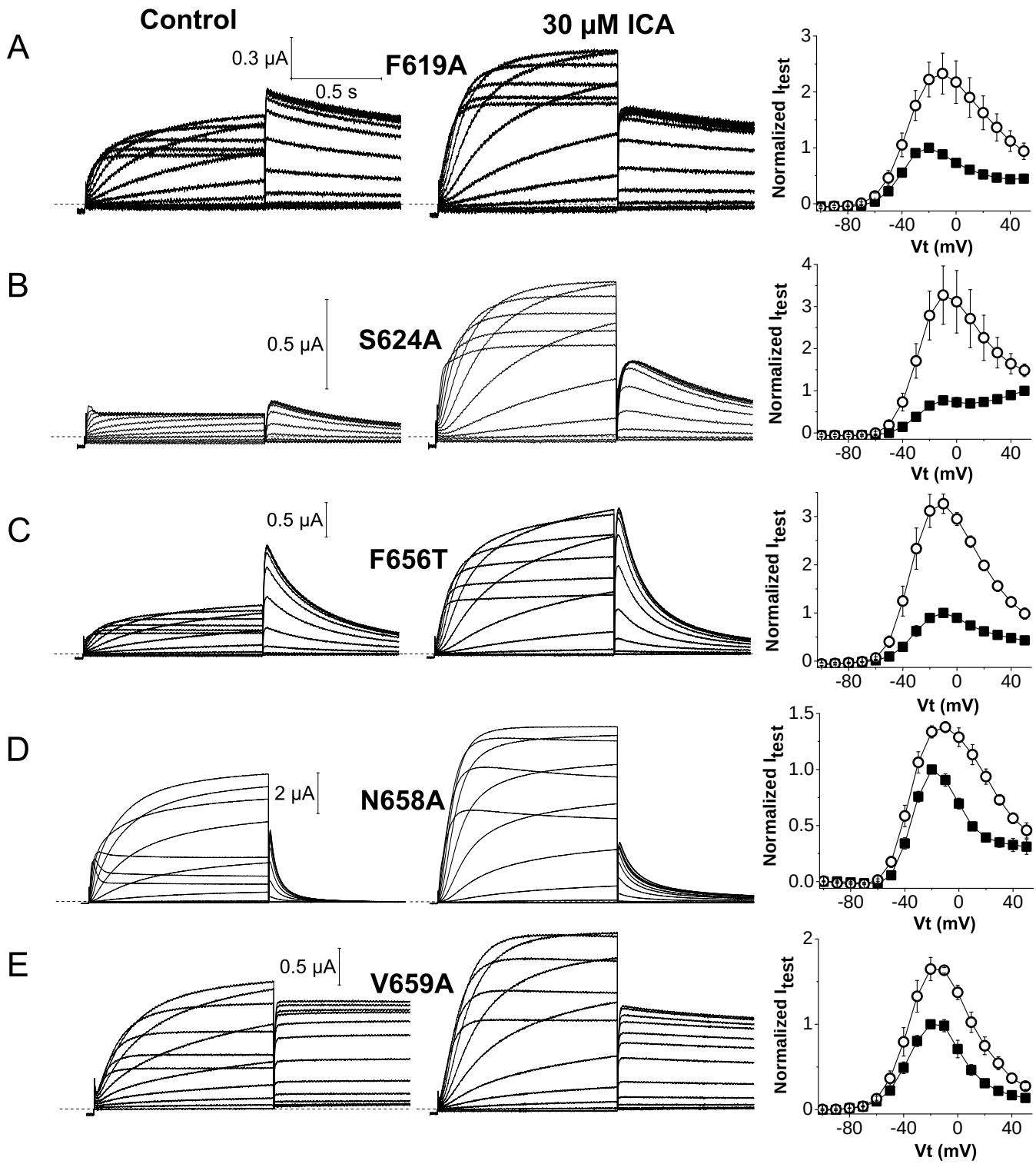

Fig. S2. Effect of ICA on hERG1 channels harboring a high impact mutation. (A-E) Left and middle panels show current traces (elicited as described in Fig.1A). Right panels show averaged I-Vt relationships for currents (Itest) measured at the end of 1-s test pulses determined before (■) and after treatment of cells with 30 μM ICA (**o**) for F619A (A), S624A (B), F656T (C), N658A (D) and V659A (E) mutant hERG1 channels.
Currents were normalized relative to the peak outward control current.

Supplementary Figure S3

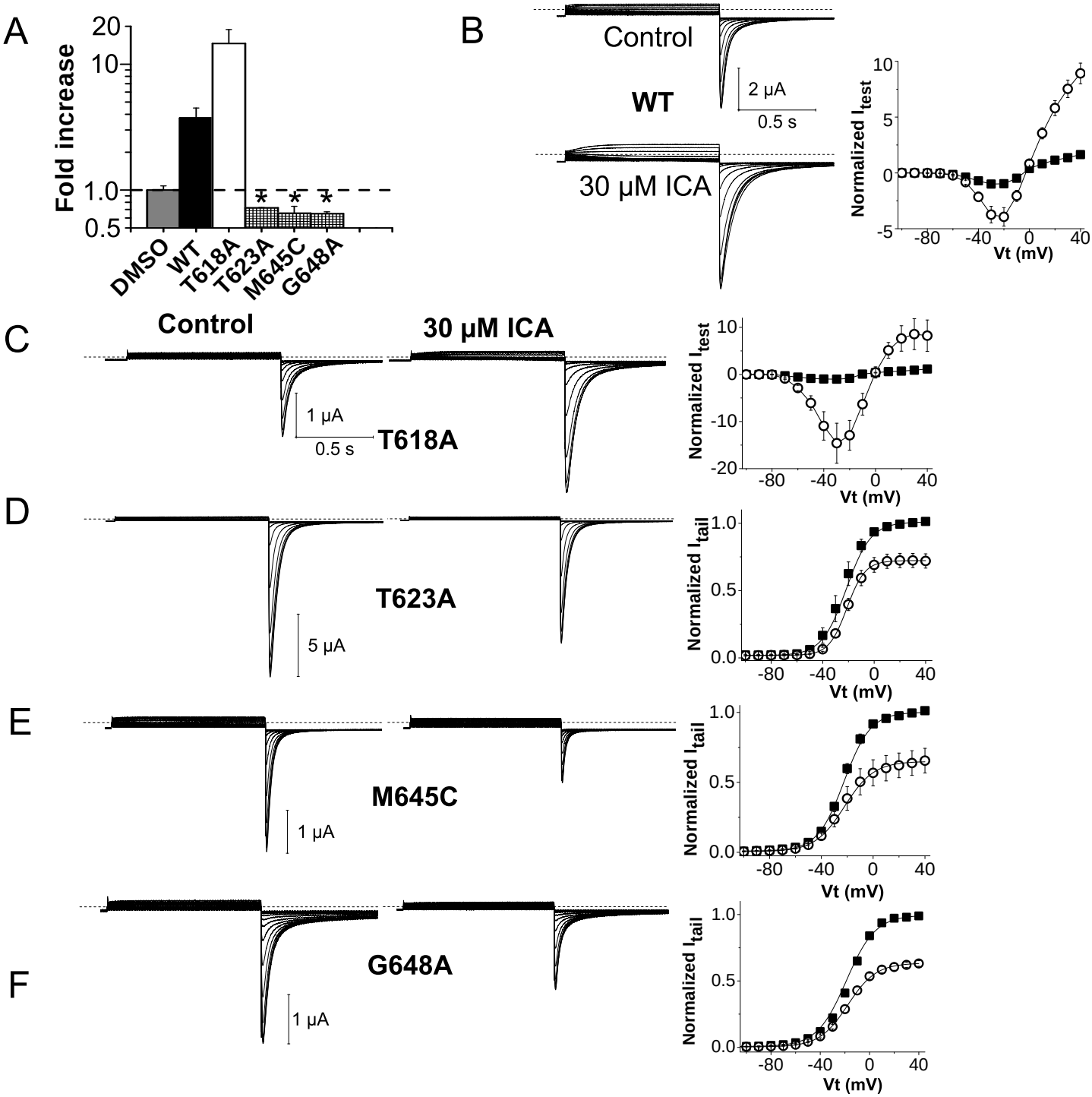

Fig. S3. Summary of the effects of ICA on mutant channels that exhibited accentuated inactivation. (A) Bar graph summarizing fold-increase in peak Itest at -30 mV (WT and T618A) and peak Itail (T623A, M645C and G648A) induced by 30 μM ICA on hERG1 channels with indicated point mutations in the pore helix (T618A, T623A) or S6 segment (M645C, G648A). Oocytes were bathed in 104 mM $[K^+]_e$ solution (see Methods) and Itail was measured at 120 mV after a 1-s test pulse to +40 mV. Vehicle control (DMSO) had no effect on currents. Mutant channels showing antagonist effect of ICA are indicated by hatched bars. *P<0.05. (B) Left panels show WT hERG1 currents recorded before (Control) and after 30 μM ICA. Step currents were elicited with 1-s pulses to a Vt that ranged from 100 to +40 mV, applied in 10 mV increments. Itail was measured at 120 mV. Right panel shows I-Vt relationship for normalized Itest at -30 mV measured before (■) and after (o) 30 μM ICA. Values were normalized to the control Itest at -30 mV. (C) Current traces (Left and middle panels) and I-Vt relationships for Itest (Right panel) for T618 hERG1 channels. (D-F) Current traces (Left and middle panels) for T623A (D), M645C (E) and G648A (F) hERG1 channels. The voltage dependence of current activation (Right panels) were determined by plotting normalized Itail measured at 120 mV as a function of Vt; data were fitted to a Boltzmann function (smooth curves).

Supplementary Figure S4

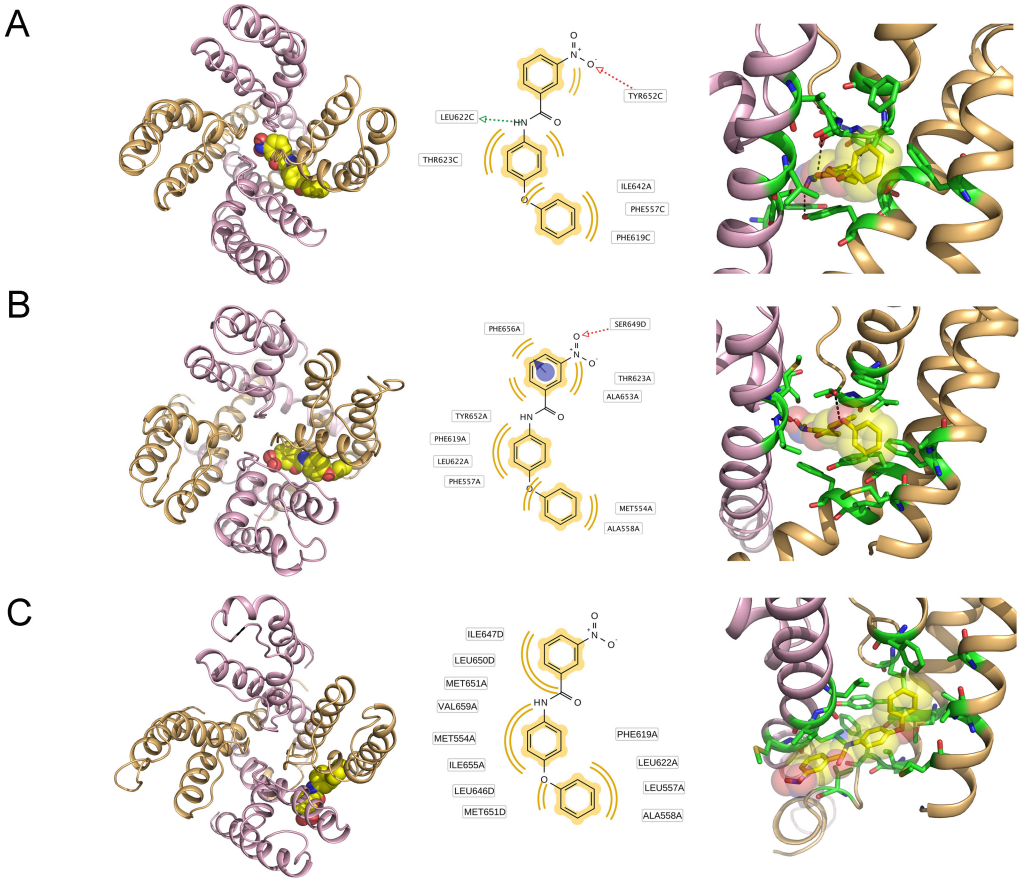

Fig. S4. Docking of ICA-105574 to WT-hERG1 and F557L hERG1 channels. (A) Left panel shows the pore module (ribbon structure) of the closed state of the WT-hERG1 channel as viewed from the extracellular space. ICA is shown in space fill. Right panel shows a close-up view of the putative drug-binding region to the closed state channel. “High impact” or other potential interacting residues are shown as stick models. Middle panel show a 2D representation of the most important interactions analyzed with LigandScout (1). Hydrogen bonds are shown as green and red dots (H-bond donor/ acceptor). Brown shades and half circles denote lipophilic and aromatic interactions. (B) ICA bound to the WT channel in the open state. The predicted binding mode for ICA include interactions with F619, F557 and Y652 via π-π stacking as well as polar interactions with selectivity filter residues. Hydrogen bonds are predicted (represented as black dots) between ICA and the backbone of L622, the side chain and/or backbone of S624, T623 and S649. (C) ICA bound to the F557L mutant channel in the closed state.

1. Wolber G & Langer T (2005) LigandScout: 3-D pharmacophores derived from protein-bound ligands and their use as virtual screening filters. J Chem Inf Model 45, 160-169.

Supplementary Figure S5

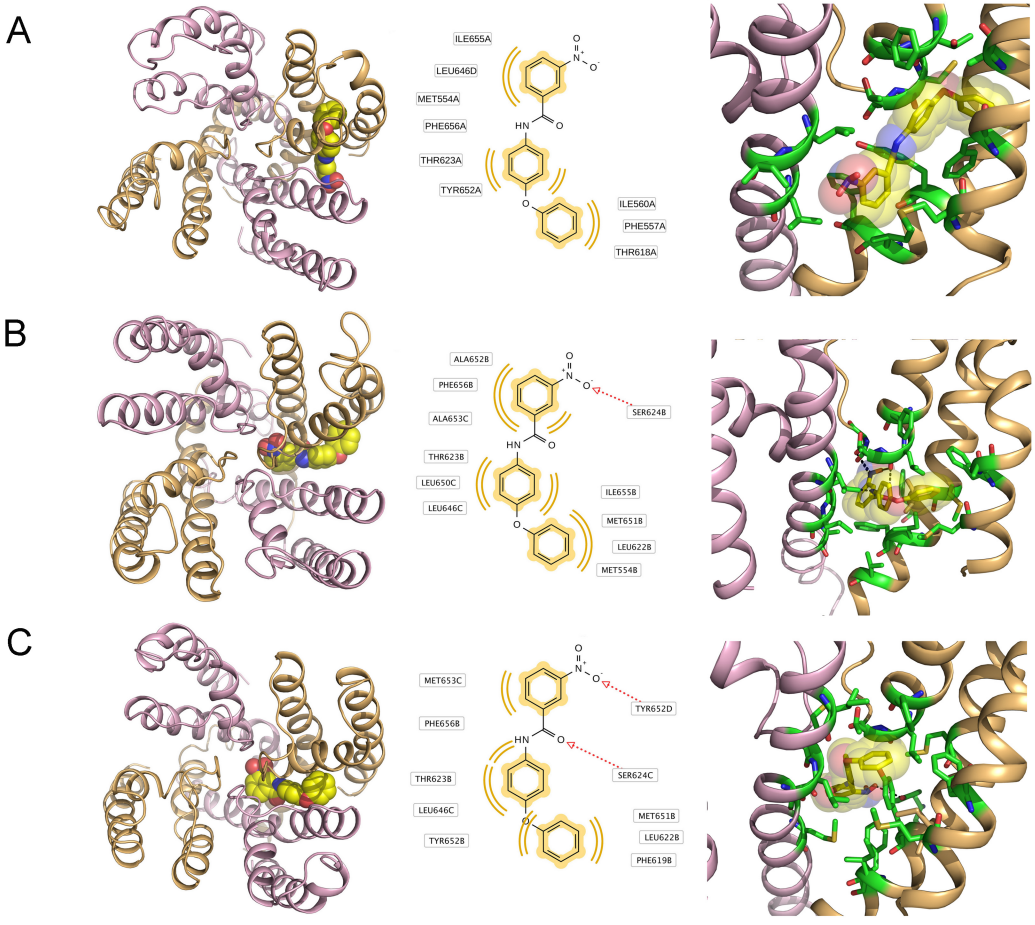

Fig. S5. Docking of ICA-105574 to the pore module of L622C, Y652A and A653M hERG1 channels in the closed state. Channel viewed from the extracellular side is depicted in Left panels, a close-up view of the putative drug-binding region is shown in the Right panels and a 2D representation of the most important interactions are indicated in the middle panels for L622C (A), Y652A (B) and A653M (C) hERG1 channels. Similar to F557L, the L622C mutation prevents the “subunit interface” binding mode observed in WT conformations and predicts ICA binding on the surface of the pore module.